RESEARCH ARTICLE

Vacuum ultraviolet photon–mediated production of $[^{18}F]F_2$

Anna Krzyczmonik[1] | **Thomas Keller**[1] | **Anna K. Kirjavainen**[1] | **Sarita Forsback**[1,2] | **Olof Solin**[1,2,3]

[1] Radiopharmaceutical Chemistry Laboratory, Turku PET Centre, University of Turku, Turku, Finland

[2] Department of Chemistry, University of Turku, Turku, Finland

[3] Accelerator Laboratory, Åbo Akademi University, Turku, Finland

Correspondence
Olof Solin, Turku PET Centre, University of Turku, Kiinamyllynkatu 4-8, FI-20520 Turku, Finland.
Email: olof.solin@abo.fi

Funding information
European Community's Seventh Framework Programm, Grant/Award Number: FP7-PEOPLE-2012-ITN-RADIOMI-316882; Academy of Finland, Grant/Award Number: 266891

The chemistry of F_2 and its derivatives are amenable to facile aliphatic or aromatic substitution, as well as electrophilic addition. The main limitation in the use of $[^{18}F]F_2$ for radiopharmaceutical synthesis is the low specific activity achieved by the traditional methods of production. The highest specific activities, 55 GBq/μmol, for $[^{18}F]F_2$ have been achieved so far by using electrical discharge in the post-target production of $[^{18}F]F_2$ gas from $[^{18}F]CH_3F$. We demonstrate that $[^{18}F]F_2$ is produced by illuminating a gas mixture of neon/F_2/$[^{18}F]CH_3F$ with vacuum ultraviolet photons generated by an excimer laser. We tested several illumination chambers and production conditions. The effects of the initial amount of $[^{18}F]F^-$, amount of carrier F_2, and number of 193-nm laser pulses at constant power were evaluated regarding radiochemical yield and specific activity. The specific activity attained for $[^{18}F]F_2$-derived $[^{18}F]NFSi$ was 10.3 ± 0.9 GBq/μmol, and the average radiochemical yield over a wide range of conditions was 6.7% from $[^{18}F]F^-$. The production can be improved by optimization of the synthesis device and procedures. The use of a commercially available excimer laser and the simplicity of the process can make this method relatively easy for adaptation in radiochemistry laboratories.

KEYWORDS
$[^{18}F]F_2$, $[^{18}F]NFSi$, electrophilic ^{18}F, excimer laser, fluorine-18, PET, radiochemistry, specific activity

1 | INTRODUCTION

Positron emission tomography (PET) is a diagnostic technique, which allows the study of biological processes in living subjects. ^{18}F is the most commonly used radionuclide in the production of PET tracers and can be introduced into a molecule by nucleophilic or electrophilic methods. Nowadays, most ^{18}F-labelled tracers are made by a nucleophilic approach because of the ready availability of nucleophilic $[^{18}F]F^-$, which is produced in high specific activity (SA) by the $^{18}O(p,n)^{18}F$ nuclear reaction in an ^{18}O-enriched water target. In contrast, electrophilic $[^{18}F]F_2$ is only produced by F_2

carrier-added methods, which lower the SA. Despite this limitation, some tracers such as $[^{18}F]CFT^1$ and $[^{18}F]EF5$ are made[2] by electrophilic fluorination.

Electrophilic fluorination is a fast way of introducing a fluorine atom into organic molecules. While F_2 can be directly used for electrophilic substitution, it can also be easily transformed into milder fluorination reagents. Presently, there are various electrophilic ^{18}F labelling reagents with different reactivities, which can be used for PET tracer production. These include $[^{18}F]XeF_2$,[3] $[^{18}F]CH_3COOF$,[4] $[^{18}F]$-N-fluorobenzenesulfonimide ($[^{18}F]NFSi$),[5] $[^{18}F]N$-fluoropyridinium salts,[6] and $[^{18}F]Selectfluor$ *bis*(triflate).[7] The use of F_2 and its derivatives allows aliphatic or aromatic substitution, as well as electrophilic addition to be performed.

Anna Krzyczmonik and Thomas Keller contributed equally to this study.

The main limitation in the use of $[^{18}F]F_2$ for tracer synthesis is the low SA achieved by the traditional methods of production. There are 2 practically useful approaches for the cyclotron production of $[^{18}F]F_2$ gas: $^{20}Ne(d,\alpha)^{18}F$ and $^{18}O(p,n)^{18}F$, which lead to SAs of 0.1 GBq/μmol[8] and 1.3 GBq/μmol,[9] respectively. In 1997, Bergman and Solin reported a method for the post-target production of $[^{18}F]F_2$ gas from $[^{18}F]CH_3F$. They applied a high-voltage discharge to perform the $^{19}F/^{18}F$ isotopic exchange and obtained $[^{18}F]F_2$ with a SA of 55 GBq/μmol.[10] Since that time, this method has been used at Turku PET Centre in the production of different tracers such as 6-$[^{18}F]$fluoro-DOPA, $[^{18}F]CFT$, and $[^{18}F]EF5$[11] for clinical use. However, the discharge method has its limitations. The high-voltage discharge (25-30 kV) creates a harsh environment in the reaction chamber resulting in the consumption of F_2 gas. Furthermore, this method requires specialized equipment, which can be difficult to install.

We propose that by using a gentler source of excitation, such as vacuum ultraviolet (VUV) photons generated by an excimer laser, we can reduce the amount of carrier F_2 gas needed for the $[^{18}F]F_2$ production and this might, in turn, result in higher SA. Since the bond-dissociation energies for fluoromethane (CH_3F) to tetra-fluoromethane (which are present in the chamber during isotopic exchange) are in a range of 260 to 219 nm,[12] the energy of the ArF excimer laser (193 nm) is sufficient to break the C–F bond. Herein, we report the proof-of-principle for the VUV illumination method for the production of $[^{18}F]F_2$.

2 | EXPERIMENTAL

2.1 | General

All organic solvents were high-performance liquid chromatography (HPLC) grade and purchased from Sigma-Aldrich (Steinheim, Germany). Potassium carbonate was also purchased from Sigma-Aldrich. Kryptofix 222 [4,7,13,16,21,24-hexaoxa-1,10-diazabicyclo[8.8.8]hexacosane] was purchased from Merck KGaA (Darmstadt, Germany). $[^{18}F]$-N-fluorobenzenesulfonimide was used as a model compound

FIGURE 2 Analytical high-performance liquid chromatography chromatograms of $[^{18}F]$-N-fluorobenzenesulfonimide. Red color denotes radioactivity, and black shows the UV signal

for the identification of the $[^{18}F]F_2$ synthesized during the experiment due to its straightforward preparation (Figure 1) and identification (Figure 2). Sodium dibenzenesulfonimide ($[^{18}F]NFSi$ precursor) was supplied by Prof Gouverneur's Group (University of Oxford, Oxford, United Kingdom).

^{18}O-enriched water for the production of ^{18}F was purchased from Rotem Industries Ltd (Arava, Israel). Gases were supplied by AGA, Linde group (Espoo, Finland).

For HPLC analysis, a Merck Hitachi LaChrom 7000 system with Hitachi D-7000 HPLC System Manager software (version 3.1.1) was used. Analyses were performed using a Waters Atlantis dC18, 3.9 × 150-mm column (Waters Corp, Milford, Massachusetts) with a gradient of H_2O and MeCN starting from 95% water to 20% water over 10 minutes with a flow of 1.5 mL/min. A wavelength of 254 nm was used for the UV detector. Radioactivity was detected with a NaI (Tl) scintillator detector (2 × 2 in; Bicron, Newbury, Ohio) placed on the HPLC column outlet.

The illumination chambers were custom made to our specifications by Finnish Special Glass Oy (Espoo, Finland). The TiO_2 reflective paint (BC-620) was purchased from Saint-Gobain Crystals (Nemours, France).

FIGURE 1 Synthesis of $[^{18}F]F_2$ from $[^{18}F]F^-_{aq}$ and subsequent synthesis of $[^{18}F]$-N-fluorobenzenesulfonimide. Yields 1 to 3 represent the respective synthesis step yields. n and m denote the respective molar amounts. As described in Bergman and Solin[10], the exchange process can be simulated by a Monte Carlo model. When the molar amount of carrier F_2 gas is in large excess compared to that of $[^{18}F]CH_3F$ (ie, n > >m) and assuming that all the bonds of the molecules in the gas mixture are broken, the exchange reaction will produce (n-3 m) moles of $[^{18}F]F_2$
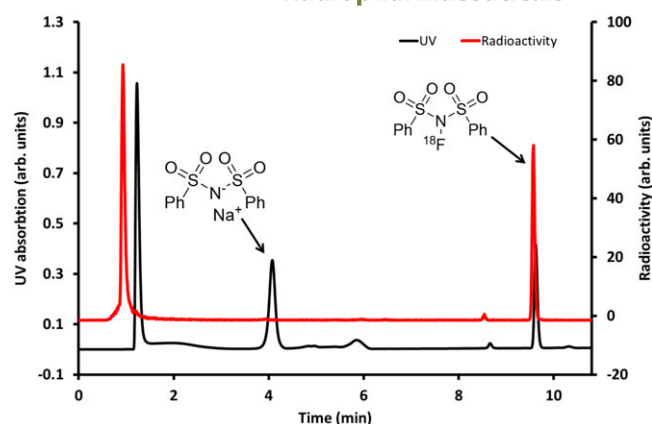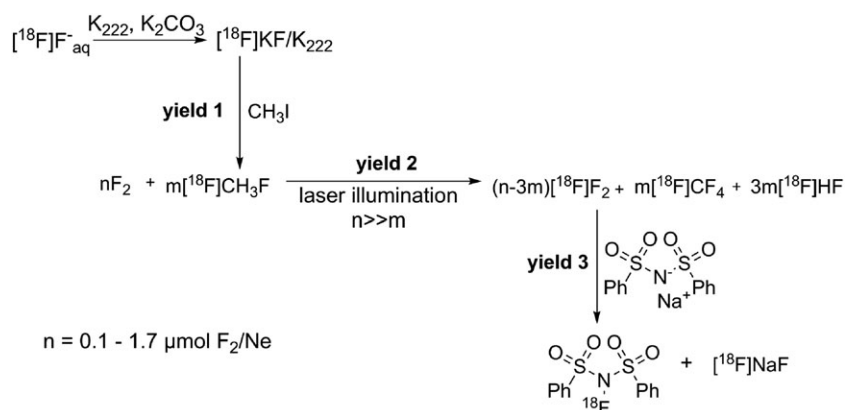
The gas chromatography column (id 0.8 cm, length 30 cm) was filled with HayeSep Q 60-80 mesh (Sigma-Aldrich, Steinheim, Germany).

2.2 | Laser

The ArF ExciStar XS laser (Coherent, Gottingen, Germany) was installed outside the hot cell. A hole was drilled in the hot cell wall, and a metal tube was used to transfer the laser beam in a helium atmosphere to the illumination chamber (Figure 3). The laser is operated in pulse mode, with 15 000, 30 000 or 60 000 pulses being used, depending on the experiment. The repetition rate (200 Hz) and energy (11-12 mJ/pulse) were kept constant for all the experiments.

2.3 | F_2 titration

The amount of carrier F_2 used in the synthesis of $[^{18}F]F_2$ was determined by iodometric titration. The mixing chamber (Figure 3A) was filled with a known pressure of Ne/0.5% F_2 gas and further filled with neon to a total pressure of 5 bar. The mixing chamber was opened to the illumination chamber, and the pressure was allowed to equilibrate
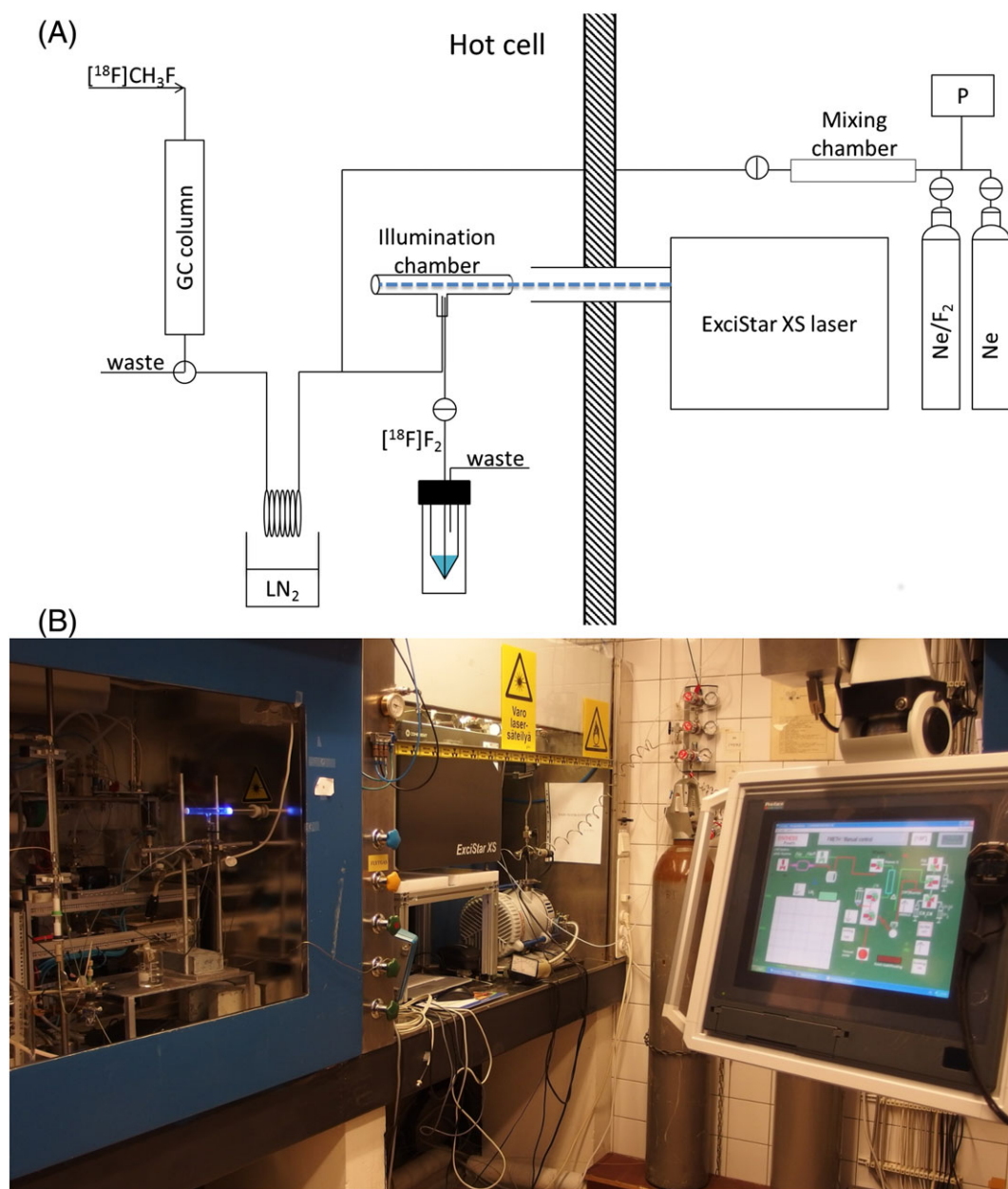

FIGURE 3 A, Schematic diagram of the apparatus for converting $[^{18}F]CH_3F$ to $[^{18}F]F_2$ using the vacuum ultraviolet laser. B, A photograph depicting the setup of the apparatus in the laboratory, from left to right; hot cell containing synthesis device, laser housed in adjacent fumehood, and the user interface

for 1 minute. The gas mixture in the illumination chamber was bubbled through 1 mL of 1M KI solution, and the chamber was flushed 3 times with neon. The resulting solution was titrated with 0.01M Na_2S_2O (when the solution color turned very pale yellow, starch indicator, 0.5 mL, was added). The amount of carrier F_2 gas was calculated from the total amount of Na_2S_2O used for titration.

2.4 | Radionuclide production by cyclotron

$[^{18}F]F^-_{aq}$ was produced via the $^{18}O(p,n)^{18}F$ reaction. ^{18}O-enriched water (800 µL) was irradiated with a beam of 17 MeV, 10 µA protons using the MGC-20 cyclotron for 5 minutes (Efremov Scientific Research Institute for Electrophysical Apparatuses [NIIEFA], Saint Petersburg, Russia). For the reactions with high activity, $[^{18}F]F^-$ was produced using the TR-19 cyclotron (Advanced Cyclotron Systems Inc Richmond, British Columbia, Canada) by irradiating ^{18}O-enriched water (3.6 mL) for 1 hour with a 19 MeV, 100 µA proton beam. An aliquot (1 mL) of the irradiated water was transferred to the synthesis apparatus for the reaction.

2.5 | Production of $[^{18}F]CH_3F$

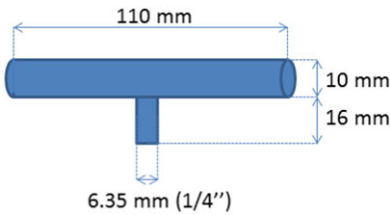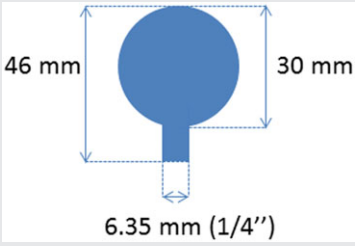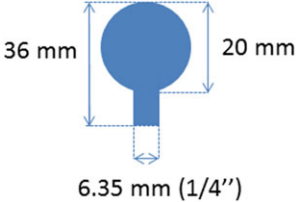The irradiated water containing the $[^{18}F]F^-_{aq}$ was transferred to a reaction vessel containing K_2CO_3 (6-8 mg), Kryptofix 222 (22-28 mg), and 1 mL of MeCN. Azeotropic distillation was conducted at 100°C for 4 minutes. Following this, a further 1 mL of MeCN was added and the drying was continued for 4 minutes. CH_3I (1.5 mmol) in 1 mL MeCN was added to the dry $[^{18}F]KF/K_{222}$ complex, and the reaction was conducted for 40 seconds at 100°C.

The resulting $[^{18}F]CH_3F$ was transferred to a 60-mL syringe and injected onto the gas chromatography column for purification. Neon was used as a carrier gas. The gas chromatography column was held at RT. A Geiger-Muller radioactivity detector, placed on the outlet of the column, monitored the elution of $[^{18}F]CH_3F$. The purified product was collected in a stainless steel loop (od 1/16", id 0.5 mm) submerged in a liquid nitrogen trap. Upon collection, the stainless steel loop was allowed to warm to room temperature for 90 seconds. Subsequently, the Ne/F_2 gas mixture, premixed to a total pressure of 5 bar as described earlier (see Section 2: F_2 titration), was used to transfer the $[^{18}F]CH_3F$ to the illumination chamber (Figure 3A). The final pressure of the gas mixture in the illumination chamber was 2.5 bar.

2.6 | $[^{18}F]F_2$ production and $[^{18}F]NFSi$ labelling

The chamber, previously filled with $[^{18}F]CH_3F/F_2/Ne$, was illuminated with the laser beam, and the resulting gas mixture

TABLE 1 Properties of illumination chambers used for the experiments

Chamber	Chamber material	Chamber shape and dimensions	Volume, cm^3	Chamber coating
A	Glass with quartz windows on ends	110 mm / 10 mm / 16 mm / 6.35 mm (1/4")	10.3	TiO_2
B	Quartz	46 mm / 30 mm / 6.35 mm (1/4")	9.8	Al
C				TiO_2
D	Quartz	36 mm / 20 mm / 6.35 mm (1/4")	4.1	Al

was bubbled, at a flow of 20 to 25 mL/min, through the solution of the NFSi precursor in 0.9 mL of MeCN and 0.1 mL of H_2O. The remaining volatile radioactive compounds were trapped in a waste bottle.

[^{18}F]NFSi was not purified. The crude solution of [^{18}F]NFSi was analyzed by analytical radioHPLC. The reported HPLC yield is an integrated yield based on the area of radioactive product peak compared to the total area of all radioactive peaks. The SA values of [^{18}F]NFSi (SA$_{[^{18}F]NFSi}$) were calculated from the analytical radioHPLC chromatograms as follows: The UV detector response was calibrated with known amounts of NFSi. The [^{18}F]NFSi fraction was collected from the HPLC outlet, the radioactivity was measured, and the area of the UV peak corresponding to NFSi was determined. The areas of the NFSi peak in the calibration and area of that in the analytical chromatogram were compared, and the amount of NFSi was calculated based on the [^{18}F]NFSi UV peak area.

During the initial screening reactions, 3 different illumination chambers were tested (Table 1). All of the chambers were coated with either an opaque layer of aluminum metal by vacuum evaporation or with TiO_2 reflective paint. In each case, a small uncoated window was left as the laser beam inlet. On chamber A, only the terminal quartz glass window was coated with paint. The chambers were connected with stainless steel Swagelok ¼" fittings and teflon ferrules.

[^{18}F]CH$_3$F was synthesized as described and transferred to the illumination chamber, and a known quantity of carrier F_2 was added (Table 2). The mixture was illuminated with 30 000 laser pulses, and the produced gas was immediately used for the synthesis of [^{18}F]NFSi. The chamber providing the highest SA$_{[^{18}F]NFSi}$ and HPLC yield was subsequently used to determine optimal number of laser pulses to promote the isotopic exchange reaction. Thus, the effect of varying the

amounts of carrier F_2 was investigated, keeping all other conditions unchanged.

The screening reactions were conducted with low starting activity (A$_{[^{18}F]F^-}$ = 3.25 ± 0.54 GBq). The conditions that resulted in the highest SA$_{[^{18}F]NFSi}$ were further used for reactions with high A$_{[^{18}F]F^-}$ (36 ± 2 GBq) to obtain high SA$_{[^{18}F]NFSi}$.

2.7 | Statistical methods

The results are reported as means ± SD of n = 3-5. All statistical analyses were performed using Microsoft Excel 2010. Differences between the HPLC yields and SA$_{[^{18}F]NFSi}$ obtained using different conditions were tested using the unpaired t-test. Differences were considered statistically significant if $P < .05$.

3 | RESULTS

[^{18}F]F$_2$ was successfully produced and subsequently used to label [^{18}F]NFSi, which was identified by analytical HPLC (Figure 2). Analysis of the crude reaction mixture showed some UV-active impurities that separated well from the product peak. Two radioactive impurities with retention times of 1 and 8.5 minutes were also observed.

3.1 | Chamber shapes and amount of laser pulses

The investigation of chamber shapes (Table 2) showed that use of the chamber A resulted in the highest HPLC yield of [^{18}F]NFSi, and hence, this chamber was chosen for all further experiments. The comparison of different coating materials (chambers B and C) (Table 2) indicated that

TABLE 2 Results of experiments conducted using different illumination chambers

Chamber	nF$_2$ (nmol)	A$_{[^{18}F]F^-}$ (GBq)	A$_{crude}$ (MBq)	SA$_{[^{18}F]NFSi}$ (GBq/µmol)	[^{18}F]NFSi HPLC Yield (%)
A	1260	3.15	142	0.04	36
A	1260	3.15	360	0.15	34
B	1280	3.75	352	0.04	15
B	1280	2.76	608	0.12	15
C	1280	3.30	451	0.04	9
C	1280	2.88	618	0.10	5
C	1280	3.60	498	0.09	5
D	1090	3.06	393	0.05	13
D	1090	3.12	333	0.04	9

Abbreviation: [^{18}F]NFSi, [^{18}F]-N-fluorobenzenesulfonimide; HPLC, high-performance liquid chromatography; SA$_{[^{18}F]NFSi}$, SA values of [^{18}F]NFSi.

The values are corrected to end of synthesis (EOS), except for the A$_{[^{18}F]F^-}$, which was measured at the start of synthesis. nF$_2$ = amount of carrier F$_2$.

KRZYCZMONIK ET AL.

WILEY
Journal of
Labelled Compounds and
Radiopharmaceuticals

191

aluminum is the better reflective material; however, the aluminum layer was also easily destroyed during the laser illumination. A comparison of the amount of laser pulses used to promote the isotopic exchange demonstrated that 30 000 pulses gave a higher yield and $SA_{[^{18}F]NFSi}$ than 15 000 pulses. However, increasing the number of laser pulses to 60 000 did not give significantly different results for either $SA_{[^{18}F]NFSi}$ ($P = .16$) or HPLC yield ($P = .051$) of [^{18}F]NFSi (Table 3). Hence, subsequent reactions were conducted with 30 000 laser pulses.

3.2 | Amount of carrier F_2 gas

Decreasing the amount of carrier F_2 led to an increase of SA $_{[^{18}F]NFSi}$. In the experiments starting with low $A_{[^{18}F]F^-}$, the highest $SA_{[^{18}F]NFSi}$ (1.2 ± 0.6 GBq/µmol) was obtained with 190 nmol of carrier F_2 (Table 4). Lowering the amount of carrier F_2 to 95 nmol did not increase the $SA_{[^{18}F]NFSi}$. The correlation between the total radioactivity of the the crude [^{18}F]NFSi solution (A_{crude}) and the $SA_{[^{18}F]NFSi}$ is shown in Figure 4.

No significant difference in the HPLC yield was observed when decreasing the amount of carrier F_2 from 1720 to 1180 nmol ($P = .096$). As the quantity of carrier was decreased from 1180 to 95 nmol, a gradual decrease in HPLC yield was observed (Table 4).

The best trial conditions (chamber A, 30 000 laser pulses and 190 nmol of carrier F_2) were used in experiments with high $A_{[^{18}F]F^-}$. These provided a $SA_{[^{18}F]NFSi}$ of 12.7 ± 1.2 GBq/µmol and a [^{18}F]NFSi HPLC yield of $13 \pm 3\%$.
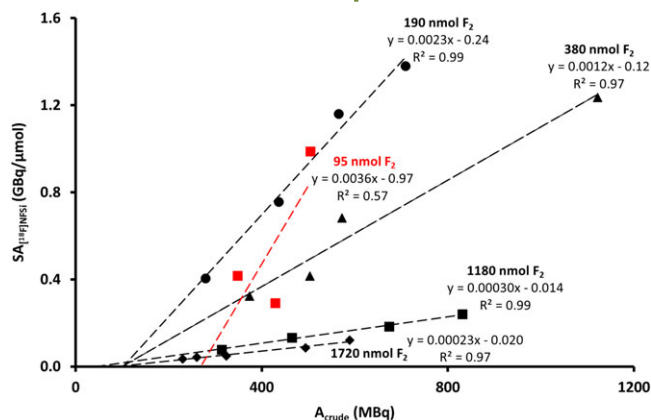

FIGURE 4 Correlations between the $SA_{[^{18}F]NFSi}$ and A_{crude}. The results for experiments with particular amounts of carrier F_2 are plotted as separate series. Linear trendlines are plotted for each series. The markers in red represent the series corresponding to the lowest amount of carrier used, where the behavior deviates from that of the others. $SA_{[^{18}F]NFSi}$, SA values of [^{18}F]NFSi

4 | DISCUSSION

A comparison of different illumination chambers showed that chamber A gave better results for the [^{18}F]NFSi labelling than the chambers B, C, or D. This can be attributed to the long path length travelled by the laser beam in the reaction gas mixture before it is reflected. The cylindrical geometry of the chamber allows direct illumination of a larger proportion of the gas, while in the spherical chambers (chambers B, C, D), most of the gas is illuminated with the reflected
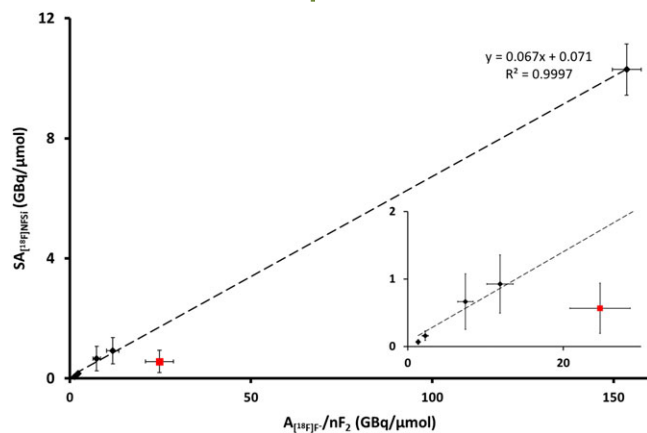
TABLE 3 Results of the experiments conducted with different amounts of pulses

Pulses	$A_{[^{18}F]F^-}$ (GBq)	A_{crude} (MBq)	$SA_{[^{18}F]NFSi}$ (GBq/µmol)	[^{18}F]NFSi HPLC Yield (%)	N
15 000	3.2 ± 0.5	420 ± 100	0.19 ± 0.12	10 ± 5	4
30 000	3.6 ± 0.5	640 ± 330	0.66 ± 0.41	23 ± 5	4
60 000	3.0 ± 0.2	260 ± 24	0.40 ± 0.08	17 ± 1	3

Abbreviation: [^{18}F]NFSi, [^{18}F]-N-fluorobenzenesulfonimide; HPLC, high-performance liquid chromatography; $SA_{[^{18}F]NFSi}$, SA values of [^{18}F]NFSi.

All experiments were done with 380 nmol of carrier F_2. The values presented are corrected to end of synthesis (EOS), except for the $A_{[^{18}F]F^-}$, which was measured at the start of synthesis.

TABLE 4 A comparison of the experiments performed with different amounts of carrier F_2

Entry	nF_2 (nmol)	$A_{[^{18}F]F^-}$ (GBq)	A_{crude} (MBq)	[^{18}F]NFSi HPLC Yield (%)	$SA_{[^{18}F]NFSi}$ (GBq/µmol)	N
1	1720	3.0 ± 0.5	380 ± 160	29 ± 2	0.07 ± 0.05	5
2	1180	3.5 ± 0.6	570 ± 230	31 ± 3	0.16 ± 0.07	4
3	380	3.6 ± 0.5	640 ± 330	23 ± 5	0.66 ± 0.41	4
4	190	2.9 ± 0.4	500 ± 180	13 ± 6	0.93 ± 0.43	4
5	95	3.1 ± 0.5	430 ± 78	5 ± 2	0.57 ± 0.37	3
6	190	35.8 ± 1.9	4100 ± 2400	13 ± 3	10.3 ± 0.9	3

The values presented are corrected to end of synthesis (EOS), except for the $A_{[^{18}F]F^-}$, which was measured at the start of synthesis. Entries 1 to 5 were conducted with a constant amount of $A_{[^{18}F]F^-}$ and a varied amount of carrier F_2. Entry 6 was conducted with 10 times higher $A_{[^{18}F]F^-}$ than the other entries.

FIGURE 5 Graph showing the linear correlation between the $SA_{[^{18}F]NFSi}$ and the theoretical maximum SA, which was calculated by dividing the $A_{[^{18}F]F^-}$ (decay corrected to EOS) by the amount of carrier F_2 (nF_2). The data series for the lowest amount of carrier used (red), where the behavior deviates from that of the others was excluded when determining the trendline. The insert in the figure is an enlargement demonstrating the excellent linear fit even at low values

photons. Although aluminum was the superior reflective material, the coating was easily destroyed by the laser beam and the illumination chamber had to be recoated with a new layer of aluminum every 3 to 4 syntheses and was hence not a practically useful coating material.

As expected, decreasing the amount of carrier F_2 increased the $SA_{[^{18}F]NFSi}$, with a maximum of 0.93 $\pm$ 0.43 GBq/µmol, which was obtained with 190 nmol of F_2. The $SA_{[^{18}F]NFSi}$ obtained in the screening reactions and conducted with various amounts of carrier F_2 were presented as a function of the A_{crude} (Figure 4). Since it is not practical to determine the radioactivity of the $[^{18}F]CH_3F$, we decided to use the A_{crude} as a measure of activity for the isotopic exchange reaction, as it accounts for the radioactivity that has been converted to either to $[^{18}F]F_2$ or $[^{18}F]HF$. Hence, the gradient of the trendlines for each data set (Figure 4) can be used as a measure of the dependence of the SA on the radioactivity of $[^{18}F]CH_3F$ used for the isotopic exchange reaction. At levels lower than 190 nmol of carrier F_2, the SA $_{[^{18}F]NFSi}$ decreased (Table 4), suggesting that during the illumination, there is a degree of consumption of the highly reactive atomic fluorine by reaction with the chamber walls or by side reactions generating $[^{18}F]$tetra-fluoromethane and $[^{18}F]$ hydrogen fluoride (Figure 1). As a result, this data series no longer followed the trend displayed in Figure 5. While the loss of atomic fluorine was lower than that of the previously published discharge method,[10] this finding suggests that there is a constant quantity of atomic fluorine that will be lost during the reaction independent of the amount of carrier F_2 added. Because the amount of carrier is decreased to lower and lower amounts, this constantly consumed quantity represents an increasingly larger proportion of the carrier F_2.

Figure 5 shows the linear correlation between the $SA_{[^{18}F]NFSi}$ and the theoretical maximum SA, which was calculated by dividing the initial $[^{18}F]$fluoride activity, decay corrected to end of synthesis (EOS), by the amount of unlabelled carrier F_2 used in the reaction. Hence, the slope of the trendline presented on the graph (0.067, $R^2 = 0.9997$) corresponds to the average radiochemical yield of 6.7% (decay corrected to EOS) of $[^{18}F]F_2$ from $[^{18}F]F^-$ for all the data sets that fit the trendline. This yield corresponds to the overall yield for the entire synthesis of $[^{18}F]NFSi$ from $[^{18}F]$fluoride and represents a combination of yields 1, 2, and 3, as shown in Figure 1. If all of these yields were 100%, the $SA_{[^{18}F]NFSi}$ would be the same as the activity of the $[^{18}F]$fluoride (A $_{[^{18}F]F^-}$) introduced divided by the molar amount of carrier (nF_2) added, ie, the units of the horizontal axis in Figure 5, and the slope of the trendline would be unity.

Since the scaling of the $SA_{[^{18}F]NFSi}$ from low to high radioactivity experiments, at a constant amount of carrier, mirrors that of the $A_{[^{18}F]F^-}$ (Table 4), it is confirmed that the total molar amount of CH_3F is essentially the same in all of the experiments.[13] Hence, using the presented conditions, the only variable that the $SA_{[^{18}F]NFSi}$ depends upon is the amount of $A_{[^{18}F]F^-}$.

5 | CONCLUSION

Vacuum ultraviolet photons were successfully used for the production of $[^{18}F]F_2$. This proof-of-concept study resulted in the production of $[^{18}F]F_2$ with a highest SA of 10.3 $\pm$ 0.9 GBq/µmol (decay corrected to EOS), a value that would be sufficient for the production of tracers such as 6-$[^{18}F]$fluoro-DOPA, $[^{18}F]CFT$, or $[^{18}F]EF5$. The use of a commercially available excimer laser and the simplicity of the process will facilitate the application of this method in different radiochemistry laboratories.

CONFLICT Of INTEREST

The authors declare that they have no conflicts of interest.

REFERENCES

1. M. Haaparanta, J. Bergman, A. Laakso, J. Hietala, O. Solin, $[^{18}F]$ß-CFT ($[^{18}F]$WIN35,428), a radioligand to study the dopamine transporter with PET: biodistribution in rats, *Synapse* 1996, 23, 321–327.

2. C. J. Koch, S. M. Evans, Non-invasive PET and SPECT imaging of tissue hypoxia using isotopically labeled 2-nitroimidazoles, *Adv. Exp. Med. Biol.* 2003, 510, 285–292.

3. G. Schrobilgen, G. Firnau, R. Chirakal, E. S. Garnett, Synthesis of [^{18}F]XeF$_2$, a novel agent for the preparation of ^{18}F-radiopharmaceuticals, *J.C.S. Chem. Comm.* 1981, 4, 198–199.

4. D. M. Jewett, J. F. Potocki, R. E. Ehrenkaufer, A gas-solid-phase microchemical method for the synthesis of acetyl hypofluorite, *J. Fluorine Chem.* 1984, 24, 477–484.

5. H. Teare, E. G. Robins, E. Årstad, S. K. Luthra, V. Gouverneur, Synthesis and reactivity of [^{18}F]-*N*-fluorobenzenesulfonimide, *Chem. Commun.* 2007, 23, 2330–2332.

6. F. Oberdorfer, E. Hofmann, W. Maier-Borst, Preparation of ^{18}F-labelled N-fluoropyridinium triflate, *J. Labelled Compd. Radiopharm.* 1988, 25, 999–1005.

7. H. Teare, E. G. Robins, A. Kirjavainen, S. Forsback, G. Sandford, O. Solin, S. K. Luthra, V. Gouverneur, Radiosynthesis and Evaluation of [^{18}F]Selectfluor bis(triflate), *Angew. Chem. Int. Ed.* 2010, 49, 6821–6824.

8. G. Blessing, H. H. Coenen, K. Franken, S. M. Qaim, Production of [^{18}F]F$_2$, H^{18}F and ^{18}F$_{aq}^-$ using the ^{20}Ne(d, α)^{18}F process, *Appl. Radiat. Isot.* 1986, 37, 1135–1139.

9. E. Hess, G. Blessing, H. H. Coenen, S. M. Qaim, Improved target system for production of high purity [^{18}F]fluorine via the ^{18}O(p,n)^{18}F reaction, *Appl. Radiat. Isot.* 2000, 52, 1431–1440.

10. J. Bergman, O. Solin, Fluorine-18-labeled fluorine gas for synthesis of tracer molecules, *Nucl. Med. Biol.* 1997, 24, 677–683.

11. S. Forsback, O. Solin, Post-target produced [^{18}F]F$_2$ in the production of PET radiopharmaceuticals, *Radiochem. Acta.* 2015, 3, 219–226.

12. B. E. Smart, In *Molecular Structure and Energetic*, (Eds. J. F. Smart, A. Greenberg), Vol. 3, VCH Publishers, Deerfield Beach, FL, 1986, pp. 141.

13. O. Solin, J. Bergman, M. Haaparanta, A. Reissell Production of ^{18}F from Water Targets. Specific Radioactivity and Anionic Contaminants, *Appl. Radiat. Isot.* 1988, 10, 1065–1071.